6 The ocean lithosphere

The age of the oceanic crust, as reflected in the magnetic striping of the ocean floor, increases with distance away from the mid-ocean ridges, indicating that the ridges are the site of generation of new oceanic crust. The volcanic rocks extruded at the surface of the ridges are exclusively basalt (mid-ocean ridge basalt or MORB) which, together with there sub-volcanic intrusive equivalents - gabbros and sheeted dykes, comprise the entire oceanic crust. The total thickness of the oceanic crust generated by mafic igneous activity at the ridges is typically about 5-7 km. The structure of oceanic crust and parts of the subcrustal lithosphere can be directly observed in some ancient orogenic belts where fragments of the oceanic lithosphere have been obducted to form *ophiolites* during collision processes, for example the Semail ophiolite in Oman.

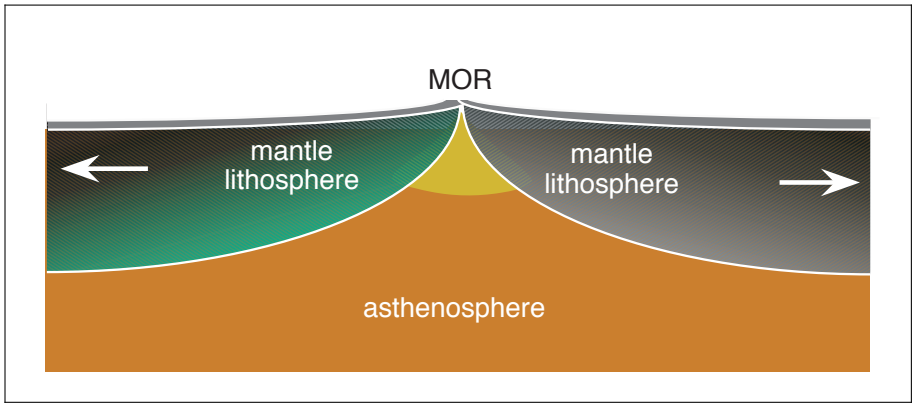

Figure 6.1 Schematic structure of the ocean lithosphere. The ocean lithosphere consists of about 6-7 km thick crust and the mantle lithosphere which thickens with age (and hence distance away from the ridge as indicated by arrows). Light stiple show the region of decompression melting beneath the ridge. The asthenosphere undergoes decompression immediately beneath the ridge.

6.1 Age, bathymetry and heatflow

In ocean lithosphere younger than about 80 Ma there is a remarkable correspondence between age of the ocean crust, the depth to the sea floor (bathymetry) and the heat flow through the lithosphere (Figure 6.1); with bathymetric depth increasing, and surface heatflow decreasing, with the $\sqrt{age}$. This correspondence between age, bathymetry and heatflow is due to time dependent changes in the thickness of the

lithosphere. Two models for the ocean lithosphere have been proposed in order to account for this relation: the *half-space model* and the *thermal plate model*.

1 The half-space model

The cooling of ocean lithosphere after formation at a ridge can be treated as a thermal conduction problem (see Chapter 3) in which a non-steady state condition (the situation at the ridge) gradually decays towards a thermally equilibrated state (as the ocean lithosphere slides away from the ridge). The analogy (Figure 6.2a) can be made with the cooling of a semi-infinite half space, which is given by:

$$\frac{T_z - T_m}{T_s - T_m} = erfc\left(\frac{z}{2\sqrt{\kappa\, t}}\right) \tag{6.1}$$

where T_z is the temperature at depth z, T_s is the temperature at the surface interface of the semi-infinite half space (which in this case is the temperature of ocean water and is taken to be 0^oC), T_m is the temperature of the half space in the initial condition and which is maintained at infinite distance for all time (in our case the temperature of the deep mantle, 1280^oC), κ is the thermal diffusivity and t is time (the error function, erf, and its compliment, $erfc$, arise commonly in analytical solutions to the heat equation and related differential equations which employ similarity variables).

The behaviour of the error function, and hence Equation 6.1, is illustrated in Figure ??b. As z tends to ∞ or t to 0 then: erfc $\left(\frac{z}{2\sqrt{\kappa\, t}}\right) \rightarrow 0$ and T_z approaches T_m. As z tends to 0 or t to ∞ then erfc $\left(\frac{z}{2\sqrt{\kappa\, t}}\right) \rightarrow 1$ and T_z approaches T_s, providing $\left(\frac{z}{2\sqrt{\kappa\, t}}\right) < 2$

From the half space model, theoretical predictions about the temporal evolution of lithospheric thickness, heat flow and bathymetry can be derived from the basic equations governing the thermal evolution of the lithosphere. Following Turcotte and Schubert (1982, p. 164-165, p. 181-182) the thickness of the lithosphere, z_l, as a function of age, t, is given by:

$$z_l = 2.32\sqrt{\kappa\, t} \tag{6.2}$$

The depth of the ocean floor beneath the ridge crest, w, at time, t, after formation is given by:

$$w = \frac{2\,\rho_m\,\alpha\,T_m}{\rho_m - \rho_w} sqrt\frac{\kappa\, t}{\pi} \tag{6.3}$$

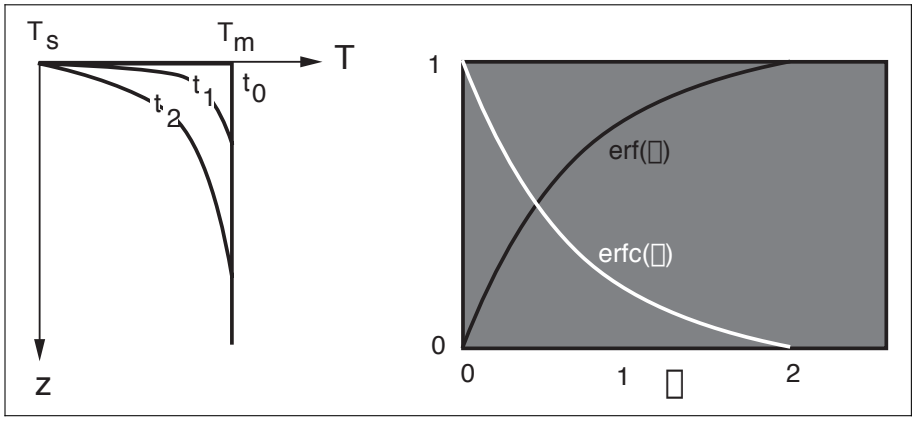

Figure 6.2 Schematic thermal structure of the ocean lithosphere treated as a problem of the cooling of a semi-infinite half space. (a) shows the thermal structure at the ridge (t_0) where asthenosphere at temperature T_m is juxtaposed with ocean waters at temperature T_s. The thermal structure at successive distances away from the ridge where cooling of the initial temperature discontinuity in the semi infinite half space has lead to thickening of the ocean lithosphere is shown by the curves t_1 and t_2. (b) shows the error function (erf) and complimentary error function ($erfc = 1 - erf$).

where α is the thermal coefficient of expansion and ρ_m and ρ_w are the density of mantle and water, respectively. The surface heat flow, q_s, at time, t, after formation is given by:

$$q_s = k\,T_m\,\frac{1}{\sqrt{\pi\,\kappa\,t}} \tag{6.4}$$

where k in the thermal conductivity.

Some interesting consequences arise from the behaviour described by these equations. For example, Equation 6.3 shows that the average depth of the ocean is proportional to its crustal age. Given a constant volume of sea water, a change in the average age and hence depth of the oceans must result in a change in sea level, which is reflected in the geological record by the extent of ocean onlap on the continents. The average age of the oceans is inversely proportional to the rate of sea floor spreading, and directly proportional to the square root of the mean age of subduction. The mean depth of the oceans, ω, as a function of the average age of subduction, t, is given by

$$\omega = \frac{1}{\tau}\int_0^{\tau} w\,dt \tag{6.5}$$

substituting for w in Eqn 2.2 gives:

$$\omega = \frac{4\,\rho_m\,\alpha_v\,T_m}{3\,(\rho_m - \rho_w)}\sqrt{\frac{\kappa\,\tau}{\pi}} \tag{6.6}$$

Secular variations in the rate of sea floor spreading, reflected in the mean age of subduction may therefore have important implications to the average height of the oceans. Indeed, this explanation has been used to account for high ocean stands during the Cretaceous (when sea level may have been up to 300 m higher than today) which correspond with periods of fast ocean floor spreading (as indicated by analysis of ocean floor magnetic anomalies).

2 The thermal plate model

The semi-inifinite half space model predicts continuous cooling (albeit at a rate that gradually decays with time) and therefore thickening of the lithosphere through time (Figure ??model). While the predictions are in remarkable agreement with the observations on bathymetry and heat flow in young ocean lithosphere these relationships appear to break down in ocean lithosphere older than about 80 Ma, when the thermal structure of the oceanic lithosphere appears to be stabilised.

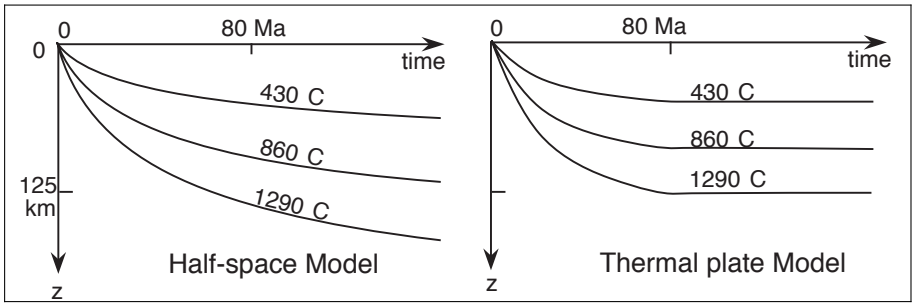

Figure 6.3 Thermal structure of the ocean lithosphere predicted by the semi-infinite half space model (a) and by the thermal plate model (b).

The semi-infinite half space model assumes that the half space is not convecting. In the earth the deep mantle is convecting, with the consequence that a convective heat flux is provided at the top of the convecting layer (see Chapter 7). The thermal plate model accounts for this apparent time independent behaviour of old oceanic lithosphere by assuming that the convection in the subjacent mantle provides sufficient heat to the base of the cooling lithosphere to stabilise the cooling once a critical thickness is reached, the observations suggest this critical thickness is about 125 km corresponding to the thickness of 80 Ma old lithosphere (Figure ??modelb). Simply stated, the oceanic plate structure is thermally stabilised when the convective heat supply to the base of the lithosphere balances heat lost through the lithosphere.

6.2 Force balance on the ocean ridge

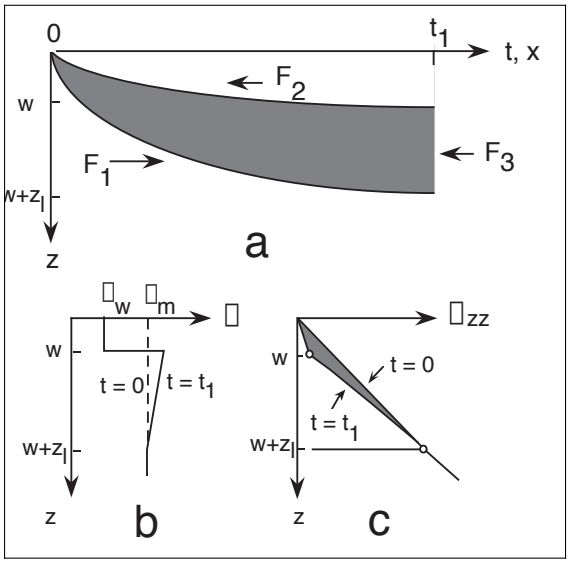

Figure 6.4 Ridge push is the force resulting from isostatically induced topographic gradients in the oceanic lithosphere. (a) shows a diagramatic representation of the force balance between a ridge and ocean lithosphere at age $t = t_1$. (b) shows the density distribution appropriate to (a). The dashed line shows the vertical density structure at $t = 0$. The solid line shows the vertical density structure at $t = t_1$. (c) shows the graphical solution to the force balance.

For young ocean lithosphere the cooling of a semi infinite half space provides an acceptable approximation and therefore Equations 6.1 - 6.3 can be used as the basis to calculate the force balance on the ocean ridge. The isostatic compensation of the oceanic lithosphere causes the youngest ocean to form a high, albeit submerged, mountain range standing out above the abyssal plains. Such profound topographic gradients necessarily lead to substantial horizontal buoyancy forces (Chapter 2), termed the ridge push. In this section we provide the methodology for calculating the magnitude of the ridge push.

Refering to Figure 6.4a the ridge push, F_R, operating on the oceanic lithosphere of age, t_1, and depth below the ridge crest, w, is given by:

$$F_R = F_1 - F_2 - F_3 \qquad (6.7)$$

which is equivalent to solving Eqn 2.3, as shown diagramatically in Figure 6.4c. Note that F_1 corresponds to the outward push of the asthenosphere beneath the mid-ocean ridge while F_2 and F_3 correspond, respectively, to the push of the water column and the old ocean lithosphere inward against the ridge.

The quantitative evaluation of Eqn 6.7 is given in the Appendix A.3. The solution of Eqn eqn 6.7 for any depth, w, below the ridge crest is shown in Figure 6.5, assuming the following physical properties α = 5 x 10^{-5}, ρ_m = 3300 kg m^{-3}, ρ_w = 1000 kg m^{-3}, $T_m = 1250^o$C and g = 10 m s^{-2}.

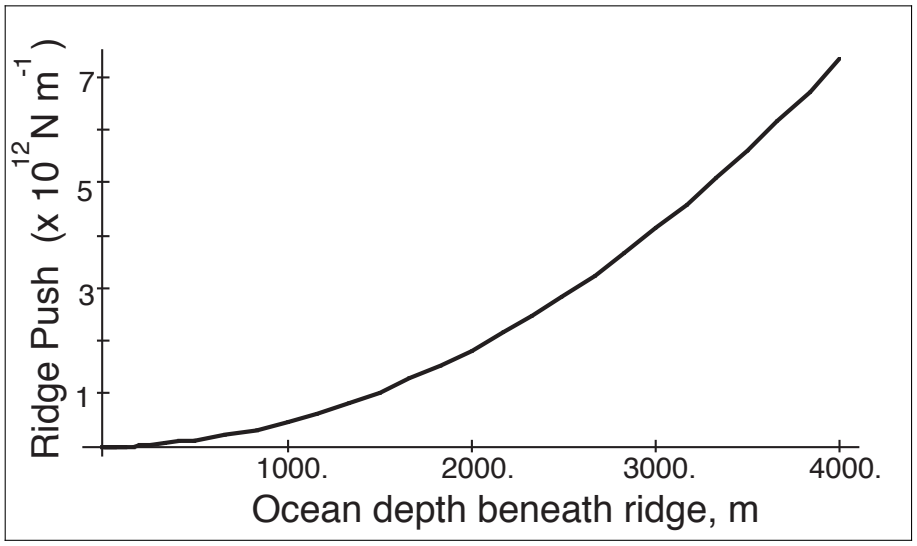

Figure 6.5 Ridge push, F_R, plotted as function of depth of ocean beneath ridge crest, w.

6.3 Formation of the oceanic crust

The ridge push resulting from the topography of the ocean floor, and the density structure within the oceanic lithosphere, provides (along with slab pull) one of the primary driving forces for lithospheric motion. The ridge push effectively maintains the constant rupturing of the oceanic lithosphere, and its separation on either side of the ridges. An important result of this rupture of the lithosphere at the ridges relates to the decompression of the underlying asthenosphere.

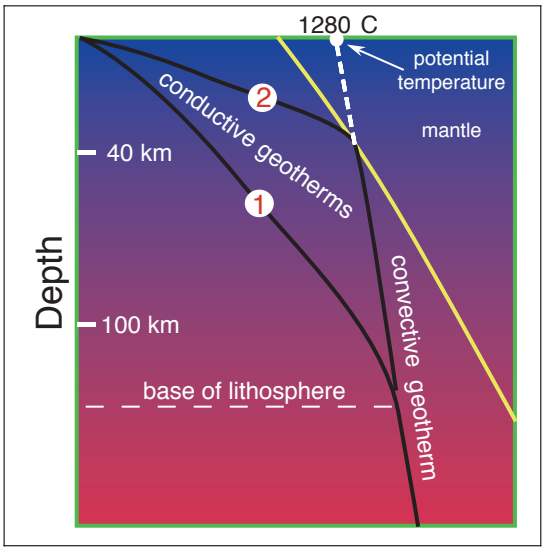

Figure 6.6 The oceanic lithosphere is characterised by its conductive geothermal gradient. The thermal gradient of the asthenosphere which is relatively well mixed (probably due to convection) is largely the isentropic temperature (adiabatic) gradient of the mantle due to volume and heat capacity (C_p) changes with changes in pressure (depth) The temperature at which this adiabatic temperature gradient extrapolates to the earth's surface is refered to as the potential temperature. Note that with the lithosphere of normal thickness (125 km), the solidus of the mantle peridotite nowhere intersects the geotherm but that on rifting of the lithosphere, the decompressed asthenosphere's adiabat intersects the solidus at about 40 km depth.

The decompression of asthenosphere beneath spreading ridges is so rapid that there is virtually no loss of heat per unit rock mass; the decompression is therefore isentropic. Since small volume increases occur during isentropic decompression there is necessarily a small decrease in the the heat content per unit volume, and hence temperature. The change in temperature with pressure at constant entropy defines the adiabat. The entropy, S, volume, V, pressure and temperature of a system are related by the Clausius - Clapeyron equation:

$$\frac{\Delta P}{\Delta T} = \frac{\Delta S}{\Delta V} \tag{6.8}$$

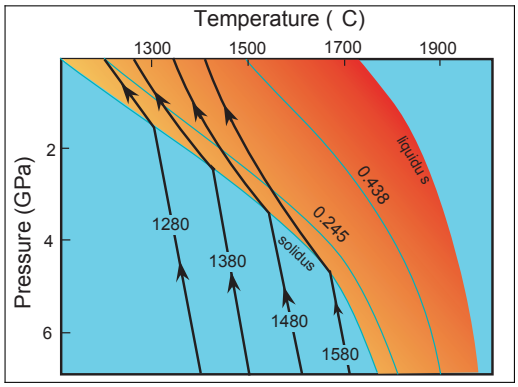

Figure 6.7 P-T diagram showing melting field of garnet peridotite and adiabatic (isentropic) decompression paths for mantle with potential temperatures of 1280^oC, 1380^oC, 1480^oC and 1580^oC, respectively (after McKenzie and Bickle, 1988).

During isentropic (adiabatic) decompression, the decrease in pressure is accompanied by only small volume increases and thus T must decrease. This adiabatic gradient is about 1^oC/km in the solid mantle. If the system becomes partly molten, then the change in volume with pressure is larger and T changes more quickly. Since the temperature of the convective mantle is not constant but lies on an adiabat we characterize it by its potential temperature (T_m), which is the projected of the adiabat to the surface of the earth (i.e., at 1 atm).

If sufficient decompression occurs, melting of the asthenosphere will take place once the adiabat passes above the solidus (Figure 6.7 and 6.8). The melt generated by this decompression has the composition of MORB and provides the parental liquid for all igneous rocks that make up the oceanic crust.

The amount of melting generated due to decompression of asthenospheric mantle beneath an active ridge segment depends entirely on the thermal structure of the asthenosphere and the melting properties of the mantle as a function of pressure. For the present day thermal structure ($T_m = 1280^oC$) the amount of melting during complete decompression, amounts to a vertical column some 7 km thick (Figure 6.8). In the past, when the internal temperature may have been considerably hotter than it is today, the column of melt generated beneath the ridges, and hence the oceanic crust, may have been significantly thicker than 7 km.

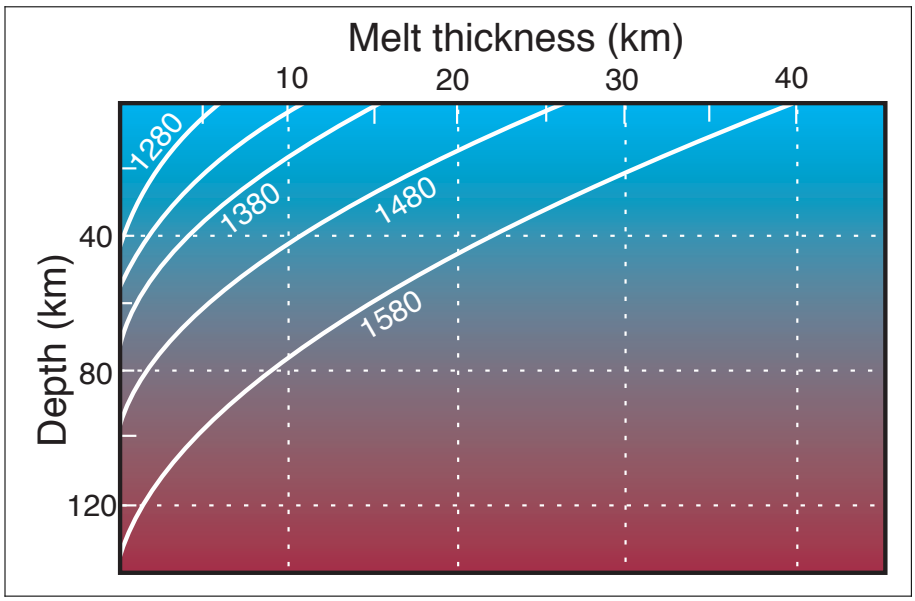

Figure 6.8 Thickness of melt (measured as a vertical column in kms) present below the given indicated depth produced by the adiabatic decompression of garnet peridotite for different potential temperatures (after McKenzie and Bickle, 1988). For the modern day mantle with a potential temperature of 1280^oC melting will not occur at depths les than about 45 km. Adiabatic decompression of the modern day mantle by the complete removal of the overlying lithospheric "lid" (for example at a spreading ridge) will result in the generation of a 7 km pile of MORB-like melt (i.e., the oceanic crust).

6.4 Coupling of the -spheres?

Equation 6.3, derived entirely from theoretical considerations, is in excellent agreement with observed bathymetry of ocean lithosphere younger than about 80 Ma. Indeed, this remarkable agreement between observations and the age-heatflow-bathymetry relationships predicted by Equations 6.1 - 6.3 provides one of the principal lynchpins of the plate tectonic paradigm and one of the most persuasive lines of argument that the lithosphere is indeed thermally stabilized. Morover, it suggests that the motion of the oceanic lithosphere is largely decoupled from the flow in the underlying asthenosphere. There is as yet no clear understanding of the location, or even the general planform of mantle upwelling in the asthenosphere. Most importantly, we have shown that there is no requirement that the ocean ridges represent the site of upwelling (Figure ??). Wherever asthenospheric upwelling occurs it is likely to modify the thermal structure of the overlying lithosphere, and the suggestion is that the thermal structure of most old oceanic lithosphere has been modified to some degree by upwelling from within the underlying mantle.